Formation-Control Stability and Communication Capacity of Multiagent Systems: A Joint Analysis

Rongrong Qian, *Member, IEEE*, Zhisheng Duan, *Senior Member, IEEE*, Yuan Qi, *Member, IEEE*, Tao Peng, *Member, IEEE*, and Wenbo Wang, *Senior Member, IEEE*

***Abstract*—The focus of this study is a joint analysis of the stability of formation control and the capacity of wireless communications between agents moving in a formation. The main results derived in this study show a connection between the second moment stability/convergence of formation control and the expected capacity of the data communications for multiagent systems in which the collective behavior of the multiple agents is dominated by formation control with random errors. More specifically, by developing a joint control-communication framework for the performance analysis, we investigate whether random errors in the formation control have a destructive influence on the data communications between agents. We prove that the expected capacity of the multiagent data communication link has a *nonvanishing* lower bound that can be evaluated through second moment performance analysis. The results from simulations indicate that the theoretical analysis provides reasonable lower bounds for different system parameters.**

***Index Terms*—Communication capacity, formation control, multiagent systems, stability.**

I. Introduction

Multiagent systems, such as multiple unmanned aerial vehicles (UAVs) and mobile robots [1], require high-quality interagent control and communication to achieve global objectives through local coordination and collaboration [1]–[10]. The capability of a multiagent system is far beyond that of a single agent, and multiagent systems have great advantages in many aspects, such as system cost, efficiency, robustness, and scalability [9], [10].

Research on multiagent systems has attracted significant attention in the control field over the past several decades [1]–[8], [12]–[16], [56] while recent years have witnessed a rapidly increasing interest in the field of communication, especially in the research of multi-UAV communications [9], [10], [17]–[22]. On the one hand, a variety of studies has focused on cooperative control problems for multiagent systems, including the cooperative control of formations (i.e., *formation control*) [1]–[5], [12]–[16], [56]. Formation control of agents is thought to be the key technology for many collaborative missions in multi-UAV, multirobot, and multisatellite systems [1], [2]. On the other hand, research efforts in the communication community have identified that one of the most critical design issues in multiagent systems is interagent communication, which faces many challenges, as these systems have to provide reliable communications between agents to transmit the traffic data of their missions, e.g., sensor, video, and communication-relaying data, with the multi-UAV system being a typical example [9], [10], [19]. Hence, great efforts have been made to address the design and implementation problems associated with multi-UAV communications [17], [19], [20] and analyze the performance of multi-UAV communications from the perspective of the ergodic capacity, outage performance, and diversity-multiplexing tradeoff [21], [22].

In addition to the two separate lines of control and communication studies, it is also crucial to understand the fundamental connections between the control and communication mechanisms of multiagent systems since they are closely related [2], [23]–[27]. The design of multiagent control laws under imperfect communication conditions, such as noise, a time-varying topology, delay, and channel uncertainty, is known for its practical significance [2], [24]–[27]. Effective control for multiagent coordination needs to be designed to ensure that the network connectivity is reliable [18]. You and Xie [27] considered the minimum data rates for stabilization and consensusability of multiagent systems. Besides, communication-aware control can facilitate networking cooperation and increase autonomy for multiagent systems [28]. It is generally difficult to carry out control and communication research jointly [29], as there is traditionally a gap between the theoretical frameworks of the two fields. That is, the modeling, analysis, and design in most control studies rely on the system dynamics [56], [58], [60], but apart from some algorithms (such as the power control

Manuscript received May 25, 2020; accepted July 12, 2020. Date of publication August 7, 2020; date of current version August 24, 2021. This work was supported in part by the National Natural Science Foundation of China under Grant 61971058, Grant 61631004, and Grant 61801048, and in part by the Beijing Natural Science Foundation under Grant L192002. Recommended by Associate Editor Murti V. Salapaka. *(Corresponding author: Yuan Qi.)*

Rongrong Qian is with the School of Artificial Intelligence, Beijing University of Posts and Telecommunications, Beijing 100876, China (e-mail: rongrongqian@bupt.edu.cn).

Zhisheng Duan is with the State Key Laboratory for Turbulence and Complex Systems, College of Engineering,Peking University, Beijing 100871, China (e-mail: duanzs@pku.edu.cn).

Yuan Qi is with the School of Electronic Engineering, Beijing University of Posts and Telecommunications, Beijing 100876, China (e-mail: qiyuan@bupt.edu.cn).

Tao Peng and Wenbo Wang are with the Wireless Signal Processing and Network Lab (Key Laboratory of Universal Wireless Communication, Ministry of Education), Beijing University of Posts and Telecommunications, Beijing 100876, China (e-mail: pengtao@bupt.edu.cn; wbwang@bupt.edu.cn).

Digital Object Identifier 10.1109/TCNS.2020.3015028

algorithm [30]), few system models in communication research use the system dynamics. Regarding formation-control multiagent systems, the joint research can take advantage of the collective behavior of agents. More specifically, these systems are self-organized, having a specific collective behavior [17], [28] governed by the formation-control dynamics that can determine the distance between every pair of agents and thus affect the performance of interagent communication. An important feature of this kind of collective behavior is that every individual agent's action is dominated by the states of other (neighboring) agents, where the state information of one agent can spread to others by means of measurement and communication, both of which are unavoidably subject to random errors [2], [48], [49]. These errors can easily affect the collective behavior of the formation control of multiagent systems, implying that these systems are prone to influence by random errors.

Therefore, in this study, we consider formation-control multiagent systems and jointly analyze the stability and capacity performance under the assumption that the formation control is corrupted by random errors. The motivations of our work are fourfold. First, capacity is a fundamental metric of communication systems, indicating the theoretical limit of the data rate at which information can be reliably transmitted over a wireless channel [57], [59]. The communication capacity between two autonomous agents (UAVs) with random trajectories was investigated in [21]. It is clear that agents can move either randomly or in organized formations [1]–[8], [12]–[16]. The study in [21] is important, but the result is not applicable to formation-control multiagent systems in which agents do not move along random trajectories. Second, analyzing the communication capacity of multiagent systems with formation control requires properly modeling the positions of the agents. The modeling here is difficult with communication-theoretic methods, and few results are available. Third, how random errors in formation control affect the communication performance of a multiagent system is unclear. A basic question is whether it is possible to maintain reliable communication in multiagent systems when the formation control is corrupted by errors. Fourth, there is a growing concern for the communication problems in the research on formation-control multiagent systems [2], [24], [25], but the capacity performance has not been considered.

The main contributions and novelty of this article can be summarized as follows.

1) We develop an analytical framework to jointly investigate the formation-control stability and communication capacity performance of multiagent systems. The framework constructs the formation-control dynamics of multiagent systems based on stochastic differential equations, and then evaluates the expected capacity of data communication links via second moment performance analysis incorporating average-consensus analytical methods (see Theor. 1). Thus, the framework attempts to reveal a connection between the control and communication performance for multiagent systems.
2) We prove that with respect to multiagent systems, the expected capacity of the data communication link can have a nonvanishing lower bound (see Theor. 2–4), although random errors easily corrupt the formation control and their accumulation leads to a divergence of the mean square of the relative center of state (see Remark 2). Because the lower bound is explicitly expressed, we can easily use its expression in the analysis and design of communication technologies for multiagent systems.

It is worth noting that many pioneering works [31]–[42] have derived important results on the performance limitations and tradeoffs of feedback control and networked control systems under certain communication conditions (constraints) by integrating control and information theories. Elia [31], Martins, and Dahleh [32] conducted remarkable studies on the fundamental performance limitations of feedback control systems via information-theoretic interpretations and extensions of Bode's integral. In the celebrated paper [33], Tatikonda and Mitter examined the observability and stabilizability of networked control systems under communication constraints by unveiling the connection between control and the traditional information-theoretic problems of source coding and channel coding. The study [34] of Nair and Evans was influential, which investigated the minimum data rate required to stabilize the control system (i.e., the data-rate theorem [35], [36]) using information-theoretic tools. In recent years, more progress on performance tradeoffs such as rate-performance and rate-cost tradeoffs has been made [41], [42]. We refer to the work [55] of Fang *et al* for an overview of the related issues. The important distinction between our work and previous studies is that we analyze the communication performance under the formation-control condition for multiagent systems, using an analytical framework different from those in the studies [31]–[42], and attempt to derive results useful to the development of communication and networking technologies for multiagent systems (e.g., multi-UAV and mobile robots systems [9]–[11]).

Notations. Let $\mathbb{R}$ and $\mathbb{C}$ denote the real and complex fields, respectively. The real part of a complex number $a \in \mathbb{C}$ is denoted by $\mathrm{re}(a)$. Vectors are set in boldface lowercase letters, and matrices in boldface capital letters. We write a_{ij} for the entry in the ith row and jth column of the matrix $\boldsymbol{A}$, and b_i for the ith entry of the vector $\boldsymbol{b}$. The zero-mean real Gaussian distribution with variance σ^2 is denoted by $\mathcal{N}(0, \sigma^2)$. $\mathbb{E}[\cdot]$ stands for the expectation operator. Let $\mathrm{diag}(\boldsymbol{A}_1, \dots, \boldsymbol{A}_k)$ denote a block diagonal matrix with matrices $\boldsymbol{A}_i, 1 \le i \le k$, being its diagonal elements, and $\mathrm{tr}(\cdot)$ be the trace of a square matrix. The superscripts T and H are the transpose and conjugate transpose, respectively. Let $\boldsymbol{I}_m$ be the $m \times m$ identity matrix and $\boldsymbol{O}_m$ be the $m \times m$ zero matrix. We use $\mathbf{1}_n \in \mathbb{R}^n$ and $\mathbf{0}_n \in \mathbb{R}^n$ to denote the all-one and all-zero vectors, respectively. Denote by $\otimes$ the Kronecker product. We write $f(t) = O(g(t))$ if positive constants c and t_0 exist such that $|f(t)| \le cg(t)$ for all $t \ge t_0$, where $g(t)$ is strictly positive.

II. Models, Definitions, and Lemmas

A. Formation-Control Multiagent Model

Consider a group of n agents moving in an m-dimensional Euclidean space with the double-integrator dynamics

$$\dot{\boldsymbol{p}}_i(t) = \boldsymbol{v}_i(t), \qquad \dot{\boldsymbol{v}}_i(t) = \boldsymbol{u}_i(t) \tag{1}$$

where $\boldsymbol{p}_i \in \mathbb{R}^m$ denotes the position of agent i, $\boldsymbol{v}_i \in \mathbb{R}^m$ is its velocity, $\boldsymbol{u}_i \in \mathbb{R}^m$ is the control input to agent i, and $i \in \{1, \ldots, n\}$. Suppose that $\boldsymbol{u}_i$ is a formation-control law expressed by [3], [44]

$$\boldsymbol{u}_i(t) = -\alpha\left(\boldsymbol{v}_i(t) - \boldsymbol{v}^*\right) - \sum_{j=1}^{n} g_{ij}\left(\beta\Delta\boldsymbol{v}_{ij}(t) + \Delta\boldsymbol{p}_{ij}(t)\right) \tag{2}$$

where $\alpha \in \mathbb{R}$ and $\beta \in \mathbb{R}$ are positive constants, $\boldsymbol{v}^* \in \mathbb{R}^m$ is the desired velocity, and $\boldsymbol{\delta}_i \in \mathbb{R}^m$ is a constant vector with all $\boldsymbol{\delta}_i$ together determining what formation shape the multiagent system will achieve. g_{ij} denotes the interaction between two distinct agents i and j, i.e., $g_{ij} = 1$ if they are connected and $g_{ij} = 0$ otherwise, whereas $g_{ii} = 0$ for all $i \in \{1, \ldots, n\}$. $\Delta\boldsymbol{v}_{ij}(t) = \boldsymbol{v}_i(t) - \boldsymbol{v}_j(t) + \boldsymbol{\eta}_{i,j,v}$ denotes the difference between the velocities of agents i and j estimated by agent i via measurement/communication, and $\Delta\boldsymbol{p}_{ij}(t) = (\boldsymbol{p}_i(t) - \boldsymbol{\delta}_i) - (\boldsymbol{p}_j(t) - \boldsymbol{\delta}_j) + \boldsymbol{\eta}_{i,j,p}$ denotes the estimated difference between the positions of agents i and j, where $\boldsymbol{\eta}_{i,j,v}$ and $\boldsymbol{\eta}_{i,j,p}$ are the normal distributed random errors (white noise) caused by measurement/communication for which the assumption of a normal distribution has been widely used in the relevant literature [2], [24], [46]. Note that the control law (2) is closely related to the multiagent consensus problem [45], allowing the system (1) to achieve the desired formation and velocity. The law (2) is a typical displacement-based control law [3], where the survey [3] categorizes the formation control into position-, displacement-, and distance-based schemes, among which the displacement-based one is moderate in terms of the system requirements.

We specify the interaction topology of the multiagent systems as follows [3]. Let $\mathcal{V} = \{1, \ldots, n\}$ be a set of n agents with $i \in \mathcal{V}$ representing agent i. A graph $\mathcal{G} = (\mathcal{V}, \mathcal{E})$ is employed to model the interaction between the agents, where $\mathcal{G}$ is an undirected graph and $\mathcal{E} \in \mathcal{V} \times \mathcal{V}$ is the edge set of paired agents. An edge $(j, i) \in \mathcal{E}$ implies that agent i is connected to agent j, i.e., $g_{ij} = 1$. For the graph $\mathcal{G}$, the adjacency matrix and Laplacian matrix are defined as $\mathcal{A} = [g_{ij}]$ and $\mathcal{L} = [l_{ij}]$, respectively, where $l_{ii} = \sum_{j \neq i} g_{ij}$ and $l_{ij} = -g_{ij}$ for $i \neq j$.

Assumption 1: Let $\lambda_1, \ldots, \lambda_n$ be the eigenvalues of $\mathcal{L}$, where λ_i denotes the ith smallest eigenvalue. $\lambda_1 \equiv 0$ since $\mathcal{L}\boldsymbol{1}_n = \boldsymbol{0}_n$, and λ_2 is the second smallest eigenvalue, known as the algebraic connectivity, which is a measure of the global connectivity for graph $\mathcal{G}$ [50]. We assume that $\lambda_2 > 0$ such that $\mathcal{G}$ is a connected graph.

By defining $\boldsymbol{r}_i(t) := \boldsymbol{p}_i(t) - \boldsymbol{\delta}_i - \boldsymbol{v}^* t$ and $\underline{\boldsymbol{v}}_i(t) := \boldsymbol{v}_i(t) - \boldsymbol{v}^*$, the system (1) can be rewritten as $\dot{\boldsymbol{r}}_i(t) = \underline{\boldsymbol{v}}_i(t)$ and $\dot{\underline{\boldsymbol{v}}}_i(t) = \boldsymbol{u}_i(t)$, respectively. Without loss of generality, we assume that $\boldsymbol{w}_{i,j}(t) := \beta\boldsymbol{\eta}_{i,j,v} + \boldsymbol{\eta}_{i,j,p} = [w_{i,j,1}(t), \ldots, w_{i,j,m}(t)]^T \in \mathbb{R}^m$, with $w_{i,j,k}(t)$ having the following properties.

1) *Independence:* $t_1 \neq t_2 \Rightarrow w_{i,j,k}(t_1)$ and $w_{i,j,k}(t_2)$ are independent. $i_1 \neq i_2$ or $j_1 \neq j_2$ or $k_1 \neq k_2 \Rightarrow w_{i_1,j_1,k_1}(t)$ and $w_{i_2,j_2,k_2}(t)$ are independent.
2) *Stationarity:* $\{w_{i,j,k}(t)\}$ is stationary, i.e., the joint distribution of $\{w_{i,j,k}(t_1 + t), \ldots, w_{i,j,k}(t_n + t)\}$ does not depend on t.
3) For all t, $w_{i,j,k}(t)$ is normally distributed with every i, j, and k, i.e., $w_{i,j,k}(t) \sim \mathcal{N}(0, \sigma^2)$, such that $\mathbb{E}[w_{i,j,k}(t)] = 0$ and $\mathbb{E}[w_{i,j,k}^2(t)] = \sigma^2$.

We then express the above relations in matrix notation as

$$\dot{\boldsymbol{x}}_i(t) = \boldsymbol{A}\boldsymbol{x}_i(t) + \boldsymbol{B}\widetilde{\boldsymbol{u}}_i(t) \tag{3}$$

$$\widetilde{\boldsymbol{u}}_i(t) = \sum_{j=1}^{n}\left[g_{ij}\boldsymbol{K}(\boldsymbol{x}_i(t) - \boldsymbol{x}_j(t) + \boldsymbol{w}_{i,j}(t))\right] \tag{4}$$

where $\boldsymbol{x}_i(t) = \left[\begin{smallmatrix}\boldsymbol{r}_i(t)\\ \underline{\boldsymbol{v}}_i(t)\end{smallmatrix}\right]$, $\boldsymbol{A} = \left[\begin{smallmatrix}\boldsymbol{O}_m & \boldsymbol{I}_m\\ \boldsymbol{O}_m & -\alpha\boldsymbol{I}_m\end{smallmatrix}\right]$, $\boldsymbol{K} = \left[\begin{smallmatrix}-\boldsymbol{I}_m\\ -\beta\boldsymbol{I}_m\end{smallmatrix}\right]$, and $\boldsymbol{B} = \left[\begin{smallmatrix}\boldsymbol{O}_m\\ \boldsymbol{I}_m\end{smallmatrix}\right]$. By letting $\boldsymbol{G} = \mathrm{diag}(\boldsymbol{g}_1^T, \ldots, \boldsymbol{g}_n^T)$ with $\boldsymbol{g}_i = [g_{i,1} \cdots g_{i,n}]^T$, $\boldsymbol{x}(t) = [\boldsymbol{x}_1^T(t) \cdots \boldsymbol{x}_n^T(t)]^T$, and $\boldsymbol{w}(t) = [\boldsymbol{w}_1^T(t) \cdots \boldsymbol{w}_n^T(t)]^T$ with $\boldsymbol{w}_i(t) = [\boldsymbol{w}_{i,1}^T(t) \cdots \boldsymbol{w}_{i,n}^T(t)]^T$, analogous to [24, eq. (4)],[25, eq. (4)], and[46, eq. (4)], we combine (3) and (4) to obtain

$$\dot{\boldsymbol{x}}(t) = (\boldsymbol{I}_n \otimes \boldsymbol{A} + \mathcal{L} \otimes \boldsymbol{B}\boldsymbol{K})\boldsymbol{x}(t) + (\boldsymbol{G} \otimes \boldsymbol{B}\boldsymbol{K})\boldsymbol{w}(t) \tag{5}$$

where $\boldsymbol{x}(t)$ includes the agent states that are related to both the position $\boldsymbol{p}_i(t)$ and velocity $\boldsymbol{v}_i(t)$ of all agents. This takes the form of a stochastic differential equation [58], from which, by applying the multidimensional Itô integral [58], we get

$$\boldsymbol{x}(t) = \int_0^t (\boldsymbol{I}_n \otimes \boldsymbol{A} + \mathcal{L} \otimes \boldsymbol{B}\boldsymbol{K})\boldsymbol{x}(s)ds + \sigma\int_0^t (\boldsymbol{G} \otimes \boldsymbol{B}\boldsymbol{K})d\mathcal{B}(s) \tag{6}$$

where $d\mathcal{B}(s) = \boldsymbol{w}(s)ds$ with $\mathcal{B}(s) = [\mathcal{B}_1(s) \cdots \mathcal{B}_{n^2m}(s)]^T$ being an n^2m-dimensional Brownian motion (see Appendix A). The error term $\sigma\int_0^t(\boldsymbol{G} \otimes \boldsymbol{B}\boldsymbol{K})d\mathcal{B}(s)$ can be well defined according to the general Itô formula [58, Th. 4.2.1].

B. Communication Model

The multiagent system should deploy a series of communication and networking technologies (e.g., ad-hoc networking techniques [11], [51], [52]) to establish and maintain efficient interagent communications that must meet the quality-of-service requirements arising from practical applications [9]–[11]. There are generally two main purposes of communications within formation-control multiagent systems, as described in detail in the following. First, *control communication* should be involved in multiagent systems to exchange $\boldsymbol{v}_j(t)$ and $\boldsymbol{p}_j(t)$ for the formation control specified by (2). Agent i is said to connect to agent j (letting $g_{ij} = 1$) if there is a control communication link established between the agents. The control communication link is bidirectional such that $g_{ij} = g_{ji}$ for $i \neq j$. Second, multiagent systems must provide *data communications* among agents to transmit traffic data related to the agents' missions, e.g., sensor, video, and communication-relaying data.

Assumption 2: The communication between any two agents is sent through a wireless radio channel and is mainly dominated by the line-of-sight component [18]; thus, the communication link established between them is a Rician fading channel. In the literature, notably in the studies of multi-UAV communications [21], [22], statistical fading models of a UAV-to-UAV link often assume that the signal propagation experiences Rician fading [43].

C. Required Definitions and Useful Lemmas

For formation-control multiagent systems, we investigate the stability-related properties in the second moment sense, defined as follows.

Definition 1 (Second Moment Stability): The system (1) with control law (2) is second moment stable, if there exist nonnegative constants $U^p_{i,j} < \infty$ and $U^v_{i,j} < \infty$ for $\forall i, j \in \mathcal{V}$ such that $\lim_{t\to\infty} \mathbb{E}[\|\boldsymbol{p}_i(t) - \boldsymbol{p}_j(t)\|_2^2] \le U^p_{i,j}$ and $\lim_{t\to\infty} \mathbb{E}[\|\boldsymbol{v}_i(t) - \boldsymbol{v}_j(t)\|_2^2] \le U^v_{i,j}$, with any given initial states $\boldsymbol{p}_i(0), \boldsymbol{p}_j(0), \boldsymbol{v}_i(0)$, and $\boldsymbol{v}_j(0)$.

Definition 2 (Second Moment Convergence): The system (1) with control law (2) is said to be second moment convergent, if $\lim_{t\to\infty} \mathbb{E}[\|\boldsymbol{p}_i(t) - \boldsymbol{p}_j(t)\|_2^2] = \|\boldsymbol{\delta}_i - \boldsymbol{\delta}_j\|_2^2$ and $\lim_{t\to\infty} \mathbb{E}[\|\boldsymbol{v}_i(t) - \boldsymbol{v}_j(t)\|_2^2] = 0 \ \forall i, j \in \mathcal{V}$ with any given initial states $\boldsymbol{p}_i(0)$, $\boldsymbol{p}_j(0)$, $\boldsymbol{v}_i(0)$, and $\boldsymbol{v}_j(0)$.

From a communication standpoint, capacity is a fundamental metric in the performance analysis of communications over wireless radio channels, leading to important insights into wireless communication and networking technologies [57]. Let us provide several lemmas useful for analyzing the capacity performance of formation-control multiagent systems.

Lemma 1 (see [21]): Suppose that the wireless radio channel is Rician fading with the parameter K, where the transmit power of the wireless signal is P_T and the channel noise has a variance P_N. If the square of the distance between the transmitter and receiver is L, then the ergodic capacity of this link can be approximated as $C_{\text{erg}} = \mathbb{E}[\mathcal{I}] \approx C_{\text{ergL}}(L)$, where

$$C_{\text{ergL}}(L) \coloneqq \frac{1}{\ln(2)} \left[\ln\left(1 + \vartheta(L)\right) - \frac{(2K+1)}{2(1+K)^2 \left(1 + \frac{1}{\vartheta(L)}\right)^2} \right]$$

with $\mathcal{I} := \log_2(1 + \vartheta(L))$ being the instantaneous capacity in which $\vartheta(L) = \frac{P_T}{P_N L^{\gamma/2}}$ is the statistically averaged signal-to-noise ratio (SNR), γ denotes the large-scale path loss exponent [57], and $C_{\text{ergL}}(L)$ is a monotonically decreasing function of L. Throughout this article, P_T and P_N are assumed to be fixed by default.

Lemma 2 (see [21]): Using Jensen's inequality, the expectation of $C_{\text{ergL}}(L)$ can be lower bounded by

$$\mathbb{E}\left[C_{\text{ergL}}(L)\right] \ge C_{\text{ergL}}\left(\mathbb{E}\left[L\right]\right)$$

in the case of $\gamma > \frac{242}{79}$.

Remark 1: The considered system can be rewritten as (6) in which the error term $\int_0^t (\boldsymbol{G} \otimes \boldsymbol{BK}) d\mathcal{B}(s)$ might increase gradually to cause the distance between the pairs of agents to increase endlessly. There exists a risk that the capacity of the data communication link between two agents might vanish (decay to zero) because the transmit power of the wireless signal is finite in practice.

With the aim of assessing the risk of the capacity vanishing, we study the capacity of the data communication link in an expectation sense, requiring the following definition.

Definition 3 (Nonvanishing Expected Capacity): With respect to the formation-control multiagent system (1) with control law (2), the expected capacity of the data communication link between agents i and j is nonvanishing if there exists a positive constant N_c such that $\lim_{t\to\infty} \mathbb{E}[C_{\text{ergL}}(\|\boldsymbol{p}_i(t) - \boldsymbol{p}_j(t)\|_2^2)] \ge N_c$.

III. Connection Between Formation-Control Stability and Communication Capacity

A. Main Results

Theorem 1: If the system (1) with formation-control law (2) is second moment stable with a positive-valued U_p, then the expected capacity of the data communication link between any two connected agents is nonvanishing, i.e., $\lim_{t\to\infty} \mathbb{E}[C_{\text{ergL}}(\|\boldsymbol{p}_i(t) - \boldsymbol{p}_j(t)\|_2^2)] \ge C_{\text{ergL}}(U_p) \ \ \forall i, j \in \mathcal{V}$, where $C_{\text{ergL}}(U_p) > 0$.

Proof: If the system is second moment stable such that $\lim_{t\to\infty} \mathbb{E}[\|\boldsymbol{p}_i(t) - \boldsymbol{p}_j(t)\|_2^2] \le U_p$, it will be true that $\lim_{t\to\infty} C_{\text{ergL}}(\mathbb{E}[\|\boldsymbol{p}_i(t) - \boldsymbol{p}_j(t)\|_2^2]) \ge C_{\text{ergL}}(U_p)$ due to the monotonicity of $C_{\text{ergL}}(L)$. Then, by Lemma 2, we can obtain $\lim_{t\to\infty} \mathbb{E}[C_{\text{ergL}}(\|\boldsymbol{p}_i(t) - \boldsymbol{p}_j(t)\|_2^2)] \ge \lim_{t\to\infty} C_{\text{ergL}} (\mathbb{E}[\|\boldsymbol{p}_i(t) - \boldsymbol{p}_j(t)\|_2^2]) \ge C_{\text{ergL}}(U_p)$. ■

For the system considered in Theorem 1, we can prove that the second moment stability is a sufficient condition to make the expected capacity of the interagent data communication link nonvanishing, but the necessity cannot be evaluated owing to the use of Jensen's inequality.

For the system (1), it is difficult to directly validate the nonvanishing expected capacity by the existing analytical methods in communication theory because evaluating the statistics of $\|\boldsymbol{p}_i(t) - \boldsymbol{p}_j(t)\|_2^2$ is intractable. The difficulty, however, can be handily resolved owing to the methods used in the average-consensus analysis of multiagent systems [24], [25] and second moment performance analysis of stochastic differential equations [47], [58]. Referring to the average-consensus studies [24], [25], let us define

$$\boldsymbol{\theta}(t) := \frac{1}{n} \sum_{i=1}^{n} \boldsymbol{x}_i(t) = \begin{bmatrix} \boldsymbol{\theta}_r(t) \\ \boldsymbol{\theta}_v(t) \end{bmatrix} \tag{7}$$

with $\boldsymbol{\theta}_r(t) := \frac{1}{n} \sum_{i=1}^{n} \boldsymbol{r}_i(t)$ and $\boldsymbol{\theta}_v(t) := \frac{1}{n} \sum_{i=1}^{n} \underline{\boldsymbol{v}}_i(t)$, whereas

$$\boldsymbol{\xi}(t) := \left[\boldsymbol{\xi}_1^T(t) \ \cdots \ \boldsymbol{\xi}_n^T(t)\right]^T \tag{8}$$

with $\boldsymbol{\xi}_i(t) := \boldsymbol{x}_i(t) - \boldsymbol{\theta}(t) = \left[\begin{smallmatrix} \boldsymbol{\xi}_{i,r}(t) \\ \boldsymbol{\xi}_{i,v}(t) \end{smallmatrix}\right] = \left[\begin{smallmatrix} \boldsymbol{r}_i(t) - \boldsymbol{\theta}_r(t) \\ \underline{\boldsymbol{v}}_i(t) - \boldsymbol{\theta}_v(t) \end{smallmatrix}\right]$.

To derive the main results, we further define

$$l_{i,j}(t) := \|\boldsymbol{p}_i(t) - \boldsymbol{p}_j(t)\|_2$$
$$L_{i,j}(t) := l_{i,j}^2(t) = \|\boldsymbol{p}_i(t) - \boldsymbol{p}_j(t)\|_2^2$$

where $l_{i,j}(t)$ represents the distance between agents i and j, $L_{i,j}(t)$ is the square of the distance, and

$$\overline{L}_{i,j}(t) := 4\mathbb{E}\left[\|\boldsymbol{\xi}(t)\|_2^2\right] + \|\boldsymbol{\delta}_i - \boldsymbol{\delta}_j\|_2^2 + 4\left\|\boldsymbol{\delta}_i - \boldsymbol{\delta}_j\right\|_2 \left\|\mathbb{E}\left[\boldsymbol{\xi}(t)\right]\right\|_2. \tag{9}$$

Lemma 3: For $L_{i,j}(t)$ and $\overline{L}_{i,j}(t)$, we have $\mathbb{E}[L_{i,j}(t)] \leq \overline{L}_{i,j}(t)$ and $\mathbb{E}[C_{\text{ergL}}(L_{i,j}(t))] \geq C_{\text{ergL}}(\overline{L}_{i,j}(t))$. Then, by the definition of $L_{i,j}(t)$, we get $\mathbb{E}[C_{\text{ergL}}(\|\boldsymbol{p}_i(t)-\boldsymbol{p}_j(t)\|_2^2)] \geq C_{\text{ergL}}(\overline{L}_{i,j}(t))$.

Proof: We first show that $L_{i,j}(t) \leq \|\boldsymbol{\xi}_{i,r}(t)\|_2^2 + \|\boldsymbol{\xi}_{j,r}(t)\|_2^2 + 2\|\boldsymbol{\xi}_{i,r}(t)\|_2\|\boldsymbol{\xi}_{j,r}(t)\|_2 + \|\boldsymbol{\delta}_i-\boldsymbol{\delta}_j\|_2^2 + 2(\boldsymbol{\delta}_i-\boldsymbol{\delta}_j)^H(\boldsymbol{\xi}_{i,r}(t)-\boldsymbol{\xi}_{j,r}(t))$, by applying the Cauchy–Schwarz–Buniakowsky inequality. Since it is easy to check that $\|\boldsymbol{\xi}_{i,r}(t)\|_2 \leq \|\boldsymbol{\xi}(t)\|_2$ and $\|\boldsymbol{\xi}_{j,r}(t)\|_2 \leq \|\boldsymbol{\xi}(t)\|_2$, we obtain $\mathbb{E}[L_{i,j}(t)] \leq 4\mathbb{E}[\|\boldsymbol{\xi}(t)\|_2^2] + \|\boldsymbol{\delta}_i-\boldsymbol{\delta}_j\|_2^2 + 2(\boldsymbol{\delta}_i-\boldsymbol{\delta}_j)^H(\mathbb{E}[\boldsymbol{\xi}_{i,r}(t)]-\mathbb{E}[\boldsymbol{\xi}_{j,r}(t)]) \leq \overline{L}_{i,j}(t)$. Then, by applying Lemma 2, we get $\mathbb{E}[C_{\text{ergL}}(L_{i,j}(t))] \geq C_{\text{ergL}}(\mathbb{E}[L_{i,j}(t)])$. Since $C_{\text{ergL}}(L)$ decreases with increasing L, $C_{\text{ergL}}(\mathbb{E}[L_{i,j}(t)]) \geq C_{\text{ergL}}(\overline{L}_{i,j}(t))$; hence, Lemma 3 is proved. ■

According to Theorem 1, Lemma 3, and the definition of $\overline{L}_{i,j}(t)$, both the second moment stability and communication capacity of the system (1) with formation-control law (2) can be evaluated if $\mathbb{E}[\|\boldsymbol{\xi}(t)\|_2^2]$ and $\|\mathbb{E}[\boldsymbol{\xi}(t)]\|_2$ are computed. Keeping this in mind, we unveil the connection between the second moment stability and communication capacity of formation-control multiagent systems.

Theorem 2: Consider the system (1) with formation-control law (2) under Assumptions 1 and 2 for which it holds that the topology graph $\mathcal{G}$ is fixed and the communication links between the connected agents are Rician fading channels with a path loss exponent of $\gamma > \frac{242}{79}$. For every pair of connected agents i and j, there exists a positive number U_{ij} such that

1) $\lim_{t\to\infty} \mathbb{E}\left[\|\boldsymbol{p}_i(t)-\boldsymbol{p}_j(t)\|_2^2\right] \leq U_{i,j}$;

2) $\lim_{t\to\infty} \mathbb{E}\left[\|\boldsymbol{v}_i(t)-\boldsymbol{v}_j(t)\|_2^2\right] \leq U_{i,j}$;

3) $\lim_{t\to\infty} \mathbb{E}\left[C_{\text{ergL}}\left(\|\boldsymbol{p}_i(t)-\boldsymbol{p}_j(t)\|_2^2\right)\right] \geq C_{\text{ergL}}(U_{ij})$

where $U_{ij} < \infty$ is defined as (21) in Appendix B. This implies that the system is second moment stable and the expected capacity of the data communication link between agents i and j is nonvanishing for $\forall i,j \in \mathcal{V}$.

Proof: See Appendix B. Note here that the preliminaries for proof are presented in Appendix A. ■

Theorem 3: Consider the system (1) with control law (2) under Assumptions 1 and 2, for which it holds that the topology graph is switched to $\mathcal{G}$ at t_0 with states $\boldsymbol{p}_i(t_0)$ and $\boldsymbol{v}_i(t_0)$, $\forall i,j \in \mathcal{V}$, and the communication links between the connected agents are Rician fading channels with a path loss exponent of $\gamma > \frac{242}{79}$. There exist positive numbers U_{ij} $\forall i,j \in \mathcal{V}$, such that the expected capacity of the data communication link related to every pair of connected agents i and j satisfies

$$C_{\text{ergL}}\left(\overline{L}_{i,j}(t-t_0)\right) - C_{\text{ergL}}(U_{ij}) = O\left(e^{\varphi_{\max}^{\text{re}}(t-t_0)}\right)$$

as t grows, where $\varphi_{\max}^{\text{re}} < 0$ is defined as (19) in Appendix B.

Proof: See Appendix C. ■

Theorem 3 is obtained to illustrate how the expected capacity of the data communication link between any two connected agents behaves as the topology of the multiagent system changes. From Theorem 3, we find that after each topology change, the formation-control law (2) allows the lower bound of $\mathbb{E}[C_{\text{ergL}}(\|\boldsymbol{p}_i(t)-\boldsymbol{p}_j(t)\|_2^2)]$, i.e., $C_{\text{ergL}}(\overline{L}_{i,j}(t-t_0))$, to approach $C_{\text{ergL}}(U_{ij})$ at a rate of $O(e^{\varphi_{\max}^{\text{re}}(t-t_0)})$, where $\varphi_{\max}^{\text{re}} < 0$ and U_{ij} depends on the topology graph $\mathcal{G}$.

In the following, the analytical result of the connection between the second moment convergence and communication capacity of formation-control multiagent systems is provided. To proceed forward, we modify the control law (2) to

$$\boldsymbol{u}_i(t) = -\alpha(\boldsymbol{v}_i(t)-\boldsymbol{v}^*) - \sum_{j=1}^{n} a(t)g_{ij}(\beta\Delta\boldsymbol{v}_{ij}(t)+\Delta\boldsymbol{p}_{ij}(t)) \quad (10)$$

where $a(\cdot):[0,\infty)\to[0,\infty)$ is a time-varying gain function that satisfies stochastic approximation-type conditions, allowing the system to be second moment convergent [23], [46]. This study does not discuss in depth how the second moment convergence is achieved; we refer to [23] and [46] for details.

Theorem 4: Consider the system (1) with control law (10) under Assumptions 1 and 2 for which it holds that the topology graph is $\mathcal{G}$ and the communication links between the connected agents are Rician fading channels with a path loss exponent of $\gamma > \frac{242}{79}$. If the system is second moment convergent, then for every pair of connected agents, the expected capacity of the data communication link is nonvanishing. More specifically

$$\lim_{t\to\infty} \mathbb{E}\left[C_{\text{ergL}}\left(\|\boldsymbol{p}_i(t)-\boldsymbol{p}_j(t)\|_2^2\right)\right] \geq C_{\text{ergL}}\left(U_{ij}^c\right) \quad (11)$$

where agents i and j are connected and $U_{ij}^c = \|\boldsymbol{\delta}_i-\boldsymbol{\delta}_j\|_2^2$.

Proof: We can validate (11) conveniently in a manner analogos to that for the proof of Theorem 1. ■

B. Discussions

We first revisit the error term $\sigma\int_0^t(\boldsymbol{G}\otimes\boldsymbol{BK})d\mathcal{B}(s)$ of $\boldsymbol{x}(t)$ in (6), which has an essential impact on the behavior of multiagent systems as shown by the following remark (see Appendix D for proof).

Remark 2: $\mathbb{E}[\|\boldsymbol{\theta}(t)\|_2^2]$ diverges (goes to infinity) with the growth rate $O(t)$ as $t\to\infty$. For clarity, we refer to $\boldsymbol{\theta}(t)$ as the *relative center of state* of the multiagent system, since $\boldsymbol{\theta}_r(t) = \frac{1}{n}\sum_{i=1}^n \boldsymbol{p}_i(t) - (\frac{1}{n}\sum_{i=1}^n \boldsymbol{\delta}_i + \boldsymbol{v}^* t)$ and $\boldsymbol{\theta}_v(t) = \frac{1}{n}\sum_{i=1}^n \boldsymbol{v}_i(t) - \boldsymbol{v}^*$ stand for the deviations of the average position $\frac{1}{n}\sum_{i=1}^n \boldsymbol{p}_i(t)$ and the average velocity $\frac{1}{n}\sum_{i=1}^n \boldsymbol{v}_i(t)$ of multiagent systems from the preferable values $\frac{1}{n}\sum_{i=1}^n \boldsymbol{\delta}_i + \boldsymbol{v}^* t$ and $\boldsymbol{v}^*$, respectively.

From Remark 2, it is intuitively clear that the error term of $\boldsymbol{x}(t)$ in (6) yields ever-increasing $\mathbb{E}[\|\boldsymbol{\theta}(t)\|_2^2]$ as t increases. This confirms that the impact of random errors exists. Nonetheless, and fortunately, this impact may not necessarily raise the risk of the capacity vanishing according to Theorems 2 and 4.

The results obtained in this study should be useful to the development of communication and networking technologies for multiagent systems (e.g., multi-UAV and mobile robots systems [9]–[11]). For example, the formation-control multiagent systems can deploy ad-hoc networking techniques to realize high-speed and wide-range data communication between agents, with the help of enabling technologies, such as the

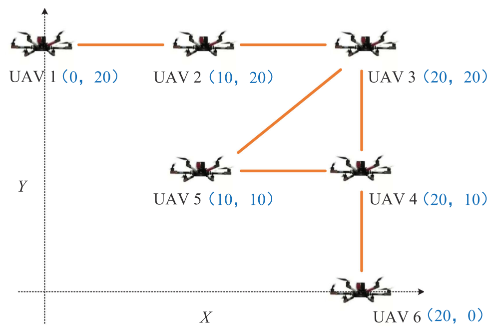

Fig. 1. Desired formation shape and interaction topology given in two-dimensional Euclidean space. The desired separations between UAVs are specified by $\boldsymbol{\delta}_1 = [0\ 20]^T$, $\boldsymbol{\delta}_2 = [10\ 20]^T$, $\boldsymbol{\delta}_3 = [20\ 20]^T$, $\boldsymbol{\delta}_4 = [20\ 10]^T$, $\boldsymbol{\delta}_5 = [10\ 10]^T$, and $\boldsymbol{\delta}_6 = [20\ 0]^T$. The Cartesian coordinate system is employed, where each $\boldsymbol{\delta}_i$ is identified with an ordered pair of coordinates (X, Y). There is a line linking UAVs i and j if they are connected.

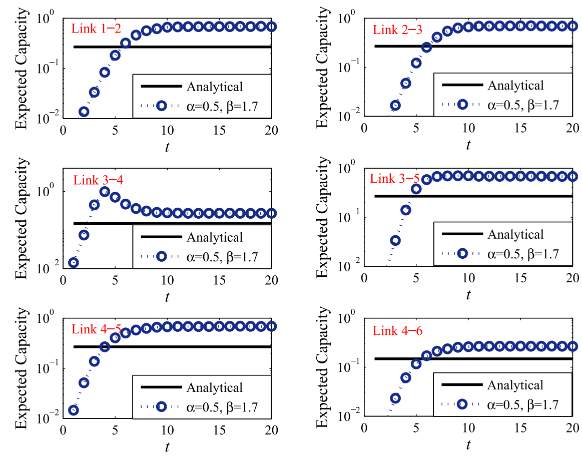

Fig. 2. Simulation results of $\mathbb{E}[C_{\text{ergL}}(\|\boldsymbol{p}_i(t) - \boldsymbol{p}_j(t)\|_2^2)]$ and analytical results of $C_{\text{ergL}}(U_{ij})$ for Theorem 2 with $\alpha = 0.5$, $\beta = 1.7$, and $\sigma = 10$.

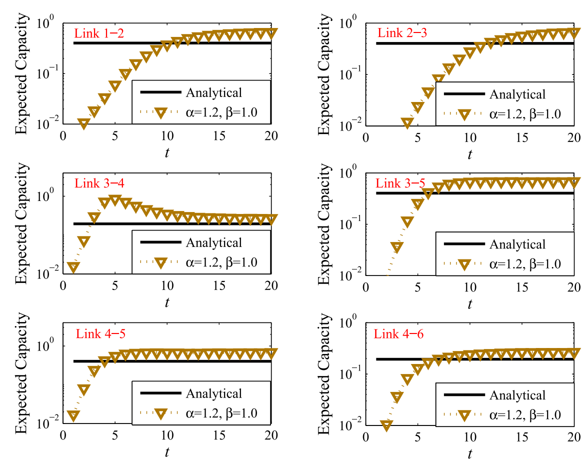

Fig. 3. Simulation results of $\mathbb{E}[C_{\text{ergL}}(\|\boldsymbol{p}_i(t) - \boldsymbol{p}_j(t)\|_2^2)]$ and analytical results of $C_{\text{ergL}}(U_{ij})$ for Theorem 2 with $\alpha = 1.2$, $\beta = 1.0$, and $\sigma = 10$.

IEEE 802.11/802.16, multihop, and routing techniques [9]–[11], [53], [54]. Herein, evaluating the communication capacity of interagent communications is a necessary task for the analysis and design of ad-hoc networking techniques, which reveals the data-rate performance (limitation) of a system and guides the data-rate-maximized design [57].

All these results should be viewed as the initial steps toward a comprehensive understanding of formation-control multiagent systems from both the control and communication perspectives. The formation-control law considered in this study is linear without delay, whereas there is a need for analogous studies on nonlinear and time-delayed formation-control laws in the future. Here, the nonlinearity and time delay make the analysis more challenging. More in-depth studies under the assumption of a time-varying topology are also necessary and important to practical multiagent systems and will be carried out by us in the future. In addition, the outage probability and outage capacity are other fundamental metrics for evaluating the communication performance of the multiagent systems of interest and should also be investigated.

IV. Simulations

To demonstrate the effectiveness of the theoretical analysis, we present simulation results for a multi-UAV system with formation control (2) in this section. The simulations performed below consider a system with six UAVs using the desired formation shape and interaction topology shown in Fig. 1. We set $K = 5$, $\gamma = 3.2$, $\frac{P_T}{P_N} = 1000$, $\boldsymbol{v}_i(0) = [0\ 0]^T$, and $\boldsymbol{p}_i(0) = [50 \times (i-1)\ 0]^T$ for all i in the simulations. For notational convenience, the wireless link between UAVs i and j is denoted by link i–j.

To illustrate Theorem 2, Figs. 2 and 3 compare the simulation results of $\mathbb{E}[C_{\text{ergL}}(\|\boldsymbol{p}_i(t) - \boldsymbol{p}_j(t)\|_2^2)]$ with the analytical results of $C_{\text{ergL}}(U_{ij})$ for different values of α and β. As can be seen from both figures, the expected capacity $\mathbb{E}[C_{\text{ergL}}(\|\boldsymbol{p}_i(t) - \boldsymbol{p}_j(t)\|_2^2)]$ gradually changes with increasing t and appears to converge to certain values that are larger than $C_{\text{ergL}}(U_{ij})$. This can be explained by Theorem 2, where $\lim_{t\to\infty} \mathbb{E}[C_{\text{ergL}}(\|\boldsymbol{p}_i(t) - \boldsymbol{p}_j(t)\|_2^2)] \geq C_{\text{ergL}}(U_{ij})$.

The simulation results for Theorem 3 shown in Figs. 4 and 5 reinforce the fact that the gap between $C_{\text{ergL}}(\overline{L}_{i,j}(t))$ and $C_{\text{ergL}}(U_{ij})$ vanishes considerably fast. From Figs. 4 and 5, we observe a finite upper bound of $\frac{C_{\text{ergL}}(\overline{L}_{i,j}(t)) - C_{\text{ergL}}(U_{ij})}{e^{\varphi_{\max}^{\text{re}} t}}$, which means that $\frac{C_{\text{ergL}}(\overline{L}_{i,j}(t)) - C_{\text{ergL}}(U_{ij})}{e^{\varphi_{\max}^{\text{re}} t}} = O(1)$. This in turn validates the statement of Theorem 3, i.e., $C_{\text{ergL}}(\overline{L}_{i,j}(t)) - C_{\text{ergL}}(U_{ij}) = O(e^{\varphi_{\max}^{\text{re}} t})$.

The simulation results of $\mathbb{E}[C_{\text{ergL}}(\|\boldsymbol{p}_i(t) - \boldsymbol{p}_j(t)\|_2^2)]$ are compared with the analytical results $C_{\text{ergL}}(U_{ij}^c)$ for Theorem 4 in Fig. 6. One observation in this comparison is worth noting: the expected capacity $\mathbb{E}[C_{\text{ergL}}(\|\boldsymbol{p}_i(t) - \boldsymbol{p}_j(t)\|_2^2)]$ apparently converges to $C_{\text{ergL}}(U_{ij}^c)$. From this observation, we can infer that the control law (10) is able to attenuate the random errors such that $\|\boldsymbol{p}_i(t) - \boldsymbol{p}_j(t)\|_2^2 \to \|\boldsymbol{\delta}_i - \boldsymbol{\delta}_j\|_2^2$, which further makes the system second moment convergent and $\mathbb{E}[C_{\text{ergL}}(\|\boldsymbol{p}_i(t) - \boldsymbol{p}_j(t)\|_2^2)] \to C_{\text{ergL}}(U_{ij}^c)$. This observation actually reflects the fact that applying Jensen's inequality yields a lower bound

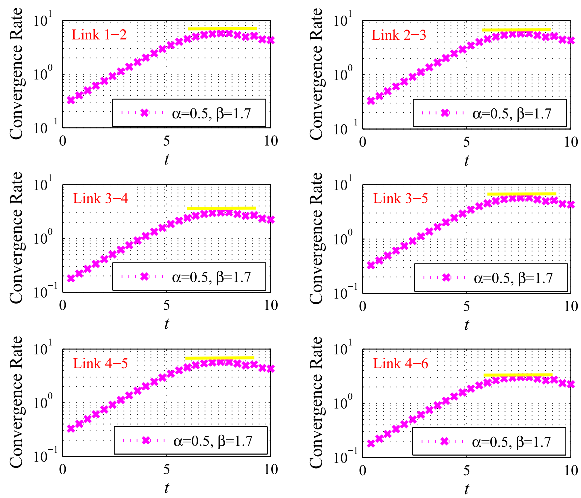

Fig. 4. Simulation results for Theorem 3 with $\alpha = 0.5$, $\beta = 1.7$, and $\sigma = 10$, letting $t_0 = 0$ without loss of generality. Convergence rate is calculated as $\frac{C_{\text{ergL}}(\overline{L}_{i,j}(t-t_0)) - C_{\text{ergL}}(U_{ij})}{e^{\varphi^{\text{re}}_{\max}(t-t_0)}}$.

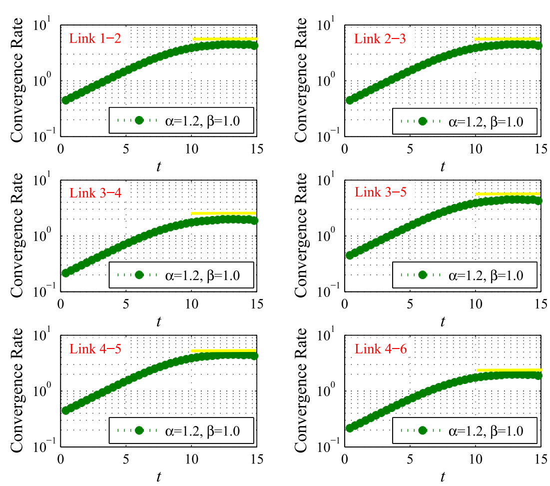

Fig. 5. Simulation results for Theorem 3 with $\alpha = 1.2$, $\beta = 1.0$, and $\sigma = 10$, letting $t_0 = 0$ without loss of generality. Convergence rate is calculated as $\frac{C_{\text{ergL}}(\overline{L}_{i,j}(t-t_0)) - C_{\text{ergL}}(U_{ij})}{e^{\varphi^{\text{re}}_{\max}(t-t_0)}}$.

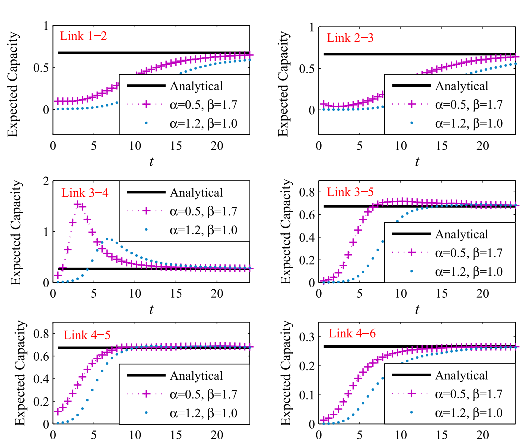

Fig. 6. Simulation results of $\mathbb{E}[C_{\text{ergL}}(\|\boldsymbol{p}_i(t) - \boldsymbol{p}_j(t)\|_2^2)]$ and analytical results of $C_{\text{ergL}}(U^c_{ij})$ for Theorem 4 with different α and β. Note that we choose $a(t) = \frac{\ln(t+2)}{t+2}$, similar to the simulation in [23].

without invoking evident looseness when deriving $\mathbb{E}[C_{\text{ergL}}(\|\boldsymbol{p}_i(t) - \boldsymbol{p}_j(t)\|_2^2)] > C_{\text{ergL}}(\overline{L}_{i,j}(t))$ in Lemma 3.

V. Conclusion

This study develops a joint control–communication framework for the performance analysis of formation-control multiagent systems. The study mainly reveals a connection between the second moment stability/convergence of the formation control and the expected capacity of data communications when the collective behavior of multiple agents is dominated by formation control with random errors.

Appendix A
Preliminaries

In this appendix, we recall some definitions of stochastic differential equations and linear systems. For further details, see, e.g., [58] and [60]. Thereafter, we provide several lemmas required by the derivations of main results.

Definition (see [58]). A Brownian motion (i.e., Wiener process) $\mathcal{B}(t)$ is characterized by the following properties:

1) $\mathcal{B}(t)$ has independent increments, i.e., $\mathcal{B}(t_1)$, $\mathcal{B}(t_2) - \mathcal{B}(t_1), \cdots, \mathcal{B}(t_n) - \mathcal{B}(t_{n-1})$ are independent for all $0 \le t_l \le \cdots \le t_n$;
2) $\mathcal{B}(t)$ has Gaussian increments, i.e., $\mathcal{B}(t+u) - \mathcal{B}(t)$ is normally distributed with mean 0 and variance u, denoted as $\mathcal{B}(t+u) - \mathcal{B}(t) \sim \mathcal{N}(0, u)$;
3) $\mathcal{B}(t)$ is the integral of a white Gaussian process [59].

Definition: The exponential function of a matrix $\boldsymbol{A}$ can be written as $e^{\boldsymbol{A}t} = \sum_{k=0}^{\infty} \frac{t^k}{k!}\boldsymbol{A}^k$ [60]. In particular, if $\boldsymbol{A} = \text{diag}(a_1, \ldots, a_k)$ is a diagonal matrix, $e^{\boldsymbol{A}t}$ will be diagonal as well, i.e., $e^{\boldsymbol{A}t} = \text{diag}(e^{a_1 t}, \ldots, e^{a_k t})$ [60].

$$\mathbb{E}\left[\left\|\int_0^t \left(\sum_{i=1}^k e^{\psi_i(t-s)}\boldsymbol{h}_i\widetilde{\boldsymbol{p}}_i^T\right) d\mathcal{B}(s)\right\|_2^2\right] \overset{(a)}{=} \mathbb{E}\left[\sum_{i=1}^k\sum_{j=1}^k \text{tr}\left(\int_0^t\int_0^t e^{\psi_i(t-s)+\psi_j^H(t-s')}\widetilde{\boldsymbol{p}}_j\boldsymbol{h}_j^T\boldsymbol{h}_i\widetilde{\boldsymbol{p}}_i^T d\mathcal{B}(s)\left(d\mathcal{B}(s')\right)^T\right)\right]$$

$$= \sum_{i=1}^k\sum_{j=1}^k \text{tr}\left(\widetilde{\boldsymbol{p}}_j\boldsymbol{h}_j^T\boldsymbol{h}_i\widetilde{\boldsymbol{p}}_i^T \int_0^t e^{\left(\psi_i+\psi_j^H\right)(t-s)}ds\right)$$

$$= \sum_{i=1}^k\sum_{j=1}^k \frac{\left(e^{\left(\psi_i+\psi_j^H\right)t} - 1\right)}{\psi_i + \psi_j^H}\text{tr}\left(\widetilde{\boldsymbol{p}}_j\boldsymbol{h}_j^T\boldsymbol{h}_i\widetilde{\boldsymbol{p}}_i^T\right). \tag{12}$$

Lemma A1: Given two real matrices $\boldsymbol{H} = [\boldsymbol{h}_1 \ \cdots \ \boldsymbol{h}_k]$ and $\boldsymbol{P} = [\widetilde{\boldsymbol{p}}_1 \ \cdots \ \widetilde{\boldsymbol{p}}_k]^T$, let $\boldsymbol{\Psi} = \text{diag}(\psi_1, \ldots, \psi_k)$ be a diagonal matrix with main diagonal entries $\psi_i \in \mathbb{C}$ and $\text{re}(\psi_i) < 0$ for all $i \in \{1, \ldots, k\}$. Then, we have $\boldsymbol{H}e^{\boldsymbol{\Psi}t}\boldsymbol{P} = \sum_{i=1}^k e^{\psi_i t}\boldsymbol{h}_i\widetilde{\boldsymbol{p}}_i^T$ and $\mathbb{E}[\|\int_0^t \boldsymbol{H}e^{\boldsymbol{\Psi}t}\boldsymbol{P}d\mathcal{B}(s)\|_2^2] = \sum_{i=1}^k\sum_{j=1}^k \frac{e^{(\psi_i+\psi_j^H)t}-1}{\psi_i+\psi_j^H}\text{tr}(\widetilde{\boldsymbol{p}}_j\boldsymbol{h}_j^T\boldsymbol{h}_i\widetilde{\boldsymbol{p}}_i^T)$, which monotonically increases with t such that $\mathbb{E}[\|\int_0^t \boldsymbol{H}e^{\boldsymbol{\Psi}t}\boldsymbol{P}d\mathcal{B}(s)\|_2^2] \le -\sum_{i=1}^k\sum_{j=1}^k \frac{\text{tr}(\widetilde{\boldsymbol{p}}_j\boldsymbol{h}_j^T\boldsymbol{h}_i\widetilde{\boldsymbol{p}}_i^T)}{\psi_i+\psi_j^H}$.

Proof: $\boldsymbol{H}e^{\boldsymbol{\Psi}t}\boldsymbol{P}=\sum_{i=1}^{k}e^{\psi_i t}\boldsymbol{h}_i\widetilde{\boldsymbol{p}}_i^T$ follows from block multiplication. A detailed procedure for deriving $\mathbb{E}[\|\int_0^t \boldsymbol{H}e^{\boldsymbol{\Psi}t}\boldsymbol{P}d\mathcal{B}(s)\|_2^2]$ can be found in (12). More specifically, we can get (a) from the properties of the trace operation. In the evaluation of the integral on the right-hand side of (a), the expectation can be calculated before carrying out integral operations, as $\mathbb{E}[d\mathcal{B}(s)(d\mathcal{B}(s))^T]=\boldsymbol{I}_k ds$ and $\mathbb{E}[d\mathcal{B}(s)(d\mathcal{B}(s'))^T]=\boldsymbol{0}_k$ for $s\neq s'$ according to the Itô isometry [58, Corollary 3.1.7]. We then have $\int_0^t e^{(\psi_i+\psi_j^H)(t-s)}ds=\frac{e^{(\psi_i+\psi_j^H)t}-1}{\psi_i+\psi_j^H}$, since $\psi_i\in\mathbb{C}$ and $\mathrm{re}(\psi_i)<0$ for each i. Substituting $\frac{e^{(\psi_i+\psi_j^H)t}-1}{\psi_i+\psi_j^H}$ for the integral, we can obtain the result of (12). Furthermore, since $\frac{d\mathbb{E}[\|\int_0^t \boldsymbol{H}e^{\boldsymbol{\Psi}t}\boldsymbol{P}d\mathcal{B}(s)\|_2^2]}{dt}=\|\boldsymbol{H}e^{\boldsymbol{\Psi}t}\boldsymbol{P}\|_2^2>0$, we find that $\mathbb{E}[\|\int_0^t \boldsymbol{H}e^{\boldsymbol{\Psi}t}\boldsymbol{P}d\mathcal{B}(s)\|_2^2]$ monotonically increases with t. ■

Lemma A2: For real numbers $\alpha,\beta>0$ and $\lambda>0$, assuming $f_+(\lambda)=-\frac{\alpha+\beta\lambda}{2}+\sqrt{\frac{(\alpha+\beta\lambda)^2}{4}-\lambda}$ and $f_-(\lambda)=-\frac{\alpha+\beta\lambda}{2}-\sqrt{\frac{(\alpha+\beta\lambda)^2}{4}-\lambda}$, there exists an eigenvalue decomposition (except for the very special case that $\lambda=\frac{(1\pm\sqrt{1-\alpha\beta})^2}{\beta^2}$) as $\begin{bmatrix}0 & 1\\ -\lambda & -(\alpha+\beta\lambda)\end{bmatrix}=\boldsymbol{\Theta}(\lambda)\boldsymbol{\Phi}(\lambda)\boldsymbol{\Theta}^{-1}(\lambda)$, where $\boldsymbol{\Theta}(\lambda)=\begin{bmatrix}1 & 1\\ f_+(\lambda) & f_-(\lambda)\end{bmatrix}$, $\boldsymbol{\Theta}^{-1}(\lambda)=\frac{1}{f_-(\lambda)-f_+(\lambda)}\begin{bmatrix}f_-(\lambda) & -1\\ -f_+(\lambda) & 1\end{bmatrix}$, and $\boldsymbol{\Phi}(\lambda)=\begin{bmatrix}f_+(\lambda) & 0\\ 0 & f_-(\lambda)\end{bmatrix}$.

Proof: Verifying this eigenvalue decomposition merely requires calculating the matrix multiplications conversely; thus, the verification is omitted here. ■

Remark A1. For positive-valued α, β, and λ, we can have $\mathrm{re}(f_-(\lambda))\leq\mathrm{re}(f_+(\lambda))\leq\varphi^{\mathrm{re}}(\lambda)<0$, where

$$\varphi^{\mathrm{re}}(\lambda):=\begin{cases}-\frac{\lambda}{(\alpha+\beta\lambda)}, & \text{if } \frac{(\alpha+\beta\lambda)^2}{4}-\lambda\geq 0\\ -\frac{\alpha+\beta\lambda}{2}, & \text{if } \frac{(\alpha+\beta\lambda)^2}{4}-\lambda<0.\end{cases}\tag{13}$$

Here, we note that $\frac{(\alpha+\beta\lambda)^2}{4}-\lambda\geq 0$ should always be true for $\alpha\beta\geq 1$; then, for $\alpha\beta<1$, it holds that $\frac{(\alpha+\beta\lambda)^2}{4}-\lambda\geq 0$ if $\lambda\in(0,\infty)\setminus(\lambda_-,\lambda_+)$ and that $\frac{(\alpha+\beta\lambda)^2}{4}-\lambda<0$ if $\lambda\in(\lambda_-,\lambda_+)$, where $\lambda_-=\frac{(1-\sqrt{1-\alpha\beta})^2}{\beta^2}$ and $\lambda_+=\frac{(1+\sqrt{1-\alpha\beta})^2}{\beta^2}$. The above analysis suggests that $\lim_{t\to\infty}|e^{f_+(\lambda)t}|=0$ and $\lim_{t\to\infty}|e^{f_-(\lambda)t}|=0$.

Lemma A3: For positive α, β, and λ, it is easy to check that $\begin{bmatrix}\boldsymbol{O}_m & \boldsymbol{I}_m\\ -\lambda\boldsymbol{I}_m & -(\alpha+\beta\lambda)\boldsymbol{I}_m\end{bmatrix}=(\boldsymbol{\Theta}(\lambda)\boldsymbol{\Phi}(\lambda)\boldsymbol{\Theta}^{-1}(\lambda))\otimes\boldsymbol{I}_m$, in light of Lemma A2.

Appendix B
Proof of Theorem 2

To complete the proof of Theorem 2, we have to derive the expressions of $\mathbb{E}[\|\boldsymbol{\xi}(t)\|_2^2]$, $\|\mathbb{E}[\boldsymbol{\xi}(t)]\|_2$, and, then, $\overline{L}_{i,j}(t)$ after obtaining Lemma 3. The starting point for evaluating $\mathbb{E}[\|\boldsymbol{\xi}(t)\|_2^2]$ and $\|\mathbb{E}[\boldsymbol{\xi}(t)]\|_2$ is the relation between $\boldsymbol{\xi}(t)$ and $\boldsymbol{x}(t)$, given as $\boldsymbol{\xi}(t)=[(\boldsymbol{I}_n-\frac{1}{n}\boldsymbol{1}_n\boldsymbol{1}_n^T)\otimes\boldsymbol{I}_{2m}]\boldsymbol{x}(t)$. Analogous to [25, eq. (6)], the dynamics (5) can be rewritten as

$$\dot{\boldsymbol{\xi}}(t)=(\boldsymbol{I}_n\otimes\boldsymbol{A}+\mathcal{L}\otimes\boldsymbol{BK})\boldsymbol{\xi}(t)+\left[\left(\boldsymbol{I}_n-\frac{1}{n}\boldsymbol{1}_n\boldsymbol{1}_n^T\right)\boldsymbol{G}\otimes\boldsymbol{BK}\right]\boldsymbol{w}(t).\tag{14}$$

Recalling that the interaction topology of the multiagent system is modeled by the undirected graph $\mathcal{G}$, we know that the Laplacian matrix $\mathcal{L}$ of $\mathcal{G}$ should be symmetric positive semidefinite, and there exists an orthogonal matrix $\boldsymbol{U}=[\frac{\boldsymbol{1}_n}{\sqrt{n}}\ \ \boldsymbol{Y}_1]=[u_{i,j}]\in\mathbb{R}^{n\times n}$ such that $\boldsymbol{U}^T\mathcal{L}\boldsymbol{U}=\boldsymbol{\Lambda}$, where $\boldsymbol{\Lambda}:=\mathrm{diag}(0,\lambda_2,\ldots,\lambda_n)$ is a diagonal matrix whose diagonal elements are the corresponding eigenvalues of $\mathcal{L}$ [25].

Define $\underline{\boldsymbol{\xi}}(t):=[\underline{\boldsymbol{\xi}}_1^T(t)\ \cdots\ \underline{\boldsymbol{\xi}}_n^T(t)]^T=(\boldsymbol{U}^T\otimes\boldsymbol{I}_{2m})\boldsymbol{\xi}(t)$. By multiplying both sides of (14) by $\boldsymbol{U}^T\otimes\boldsymbol{I}_{2m}$, we get

$$\dot{\underline{\boldsymbol{\xi}}}(t)=(\boldsymbol{I}_n\otimes\boldsymbol{A}+\boldsymbol{\Lambda}\otimes\boldsymbol{BK})\underline{\boldsymbol{\xi}}(t)+\left[\begin{bmatrix}\boldsymbol{0}_n^T\\ \boldsymbol{Y}_1^T\boldsymbol{G}\end{bmatrix}\otimes\boldsymbol{BK}\right]\boldsymbol{w}(t)$$

which follows from the fact that $\boldsymbol{I}_n-\frac{1}{n}\boldsymbol{1}_n\boldsymbol{1}_n^T=\boldsymbol{Y}_1\boldsymbol{Y}_1^T$ and $\boldsymbol{U}^T(\boldsymbol{I}_n-\frac{1}{n}\boldsymbol{1}_n\boldsymbol{1}_n^T)=[\boldsymbol{0}_n\ \ \boldsymbol{Y}_1]^T$.

Since $\underline{\boldsymbol{\xi}}_1\equiv\boldsymbol{0}_{2m}$ [25], we let $\boldsymbol{\zeta}(t):=[\underline{\boldsymbol{\xi}}_2^T(t)\ \cdots\ \underline{\boldsymbol{\xi}}_n^T(t)]^T$ to have

$$\dot{\boldsymbol{\zeta}}(t)=\underline{\boldsymbol{A}}\boldsymbol{\zeta}(t)+\underline{\boldsymbol{B}}\boldsymbol{w}(t)\tag{15}$$

where $\underline{\boldsymbol{A}}=\boldsymbol{I}_{n-1}\otimes\boldsymbol{A}+\boldsymbol{\Lambda}_1\otimes\boldsymbol{BK}$ with $\boldsymbol{\Lambda}_1:=\mathrm{diag}(\lambda_2,\ldots,\lambda_n)$, and $\underline{\boldsymbol{B}}=\boldsymbol{Y}_1^T\boldsymbol{G}\otimes\boldsymbol{BK}$. This yields

$$\boldsymbol{\zeta}(t)=e^{\underline{\boldsymbol{A}}t}\boldsymbol{\zeta}(0)+\sigma\int_0^t e^{\underline{\boldsymbol{A}}(t-s)}\underline{\boldsymbol{B}}d\mathcal{B}(s).\tag{16}$$

Noting that $\underline{\boldsymbol{A}}=\mathrm{diag}(\boldsymbol{A}+\lambda_2\boldsymbol{BK},\ldots,\boldsymbol{A}+\lambda_n\boldsymbol{BK})$, where $\boldsymbol{A}+\lambda\boldsymbol{BK}=\begin{bmatrix}\boldsymbol{O}_m & \boldsymbol{I}_m\\ -\lambda\boldsymbol{I}_m & -(\alpha+\beta\lambda)\boldsymbol{I}_m\end{bmatrix}$. By Lemma A3, we have $\underline{\boldsymbol{A}}=\boldsymbol{Q}\widehat{\boldsymbol{A}}\boldsymbol{Q}^{-1}$, where $\boldsymbol{Q}=\mathrm{diag}(\boldsymbol{\Theta}(\lambda_2),\ldots,\boldsymbol{\Theta}(\lambda_n))\otimes\boldsymbol{I}_m$, $\boldsymbol{Q}^{-1}=\mathrm{diag}(\boldsymbol{\Theta}^{-1}(\lambda_2),\ldots,\boldsymbol{\Theta}^{-1}(\lambda_n))\otimes\boldsymbol{I}_m$, and $\widehat{\boldsymbol{A}}=\mathrm{diag}(\boldsymbol{\Phi}(\lambda_2),\ldots,\boldsymbol{\Phi}(\lambda_n))\otimes\boldsymbol{I}_m$. These give rise to $e^{\underline{\boldsymbol{A}}t}=\boldsymbol{Q}e^{\widehat{\boldsymbol{A}}t}\boldsymbol{Q}^{-1}$ [60, eq. (3.51)], where $e^{\widehat{\boldsymbol{A}}t}=\mathrm{diag}(\begin{bmatrix}e^{f_+(\lambda_2)t} & 0\\ 0 & e^{f_-(\lambda_2)t}\end{bmatrix},\ldots,\begin{bmatrix}e^{f_+(\lambda_n)t} & 0\\ 0 & e^{f_-(\lambda_n)t}\end{bmatrix})\otimes\boldsymbol{I}_m$.

Applying the expectation to (16) and using the properties of the Itô integral [58] yields $\mathbb{E}[\boldsymbol{\zeta}(t)]=e^{\underline{\boldsymbol{A}}t}\boldsymbol{\zeta}(0)=\boldsymbol{Q}e^{\widehat{\boldsymbol{A}}t}\boldsymbol{Q}^{-1}\boldsymbol{\zeta}(0)$, which decreases toward a zero vector in the time limit as $\lim_{t\to\infty}\mathbb{E}[\boldsymbol{\zeta}(t)]=\lim_{t\to\infty}e^{\underline{\boldsymbol{A}}t}\boldsymbol{\zeta}(0)=\boldsymbol{0}_{(n-1)m}$. To carry the analysis further, let us consider the Euclidean norm of $\boldsymbol{\zeta}(t)$. Specifically, we define and get

$$E_\zeta(t):=\mathbb{E}\left[\|\boldsymbol{\zeta}(t)\|_2^2\right]=E_\zeta^D(t)+E_\zeta^N(t)$$

where $E_\zeta^D(t):=\|\mathbb{E}[\boldsymbol{\zeta}(t)]\|_2^2=\|\boldsymbol{Q}e^{\widehat{\boldsymbol{A}}t}\boldsymbol{Q}^{-1}\boldsymbol{\zeta}(0)\|_2^2$, and

$$E_\zeta^N(t):=\sigma^2\mathbb{E}\left[\left\|\int_0^t e^{\underline{\boldsymbol{A}}(t-s)}\left(\boldsymbol{Y}_1^T\boldsymbol{G}\otimes\boldsymbol{BK}\right)d\mathcal{B}(s)\right\|_2^2\right].$$

Furthermore, by substituting $[\psi_1\ \cdots\ \psi_{2(n-1)m}]^T=[f_+(\lambda_2)\ \ f_-(\lambda_2)\ \cdots\ f_+(\lambda_n)\ \ f_-(\lambda_n)]^T\otimes\boldsymbol{1}_m$, $\boldsymbol{H}=\boldsymbol{Q}$, and $\boldsymbol{P}=\boldsymbol{Q}^{-1}\boldsymbol{\zeta}(0)$ into Lemma A1, we can compute $E_\zeta^D(t)$ as

$$E_\zeta^D(t)=\sigma^2\sum_{i=1}^{2(n-1)m}\sum_{j=1}^{2(n-1)m}e^{\left(\psi_i+\psi_j^H\right)t}\mathrm{tr}\left(\widetilde{\boldsymbol{p}}_j\boldsymbol{h}_j^T\boldsymbol{h}_i\widetilde{\boldsymbol{p}}_i^T\right).$$

Analogously, through substituting $[\psi_1\ \cdots\ \psi_{2(n-1)m}]^T=[f_+(\lambda_2)\ \ f_-(\lambda_2)\ \cdots\ f_+(\lambda_n)\ \ f_-(\lambda_n)]^T\otimes\boldsymbol{1}_m$, $\boldsymbol{H}=\boldsymbol{Q}$, and

$\boldsymbol{P} = \boldsymbol{Q}^{-1}(\boldsymbol{Y}_1^T\boldsymbol{G}\otimes \boldsymbol{BK})$ into Lemma A1, $E_\zeta^N(t)$ can be expressed as

$$E_\zeta^N(t) = \sigma^2 \sum_{i=1}^{2(n-1)m}\sum_{j=1}^{2(n-1)m} \frac{e^{\left(\psi_i+\psi_j^H\right)t}-1}{\psi_i+\psi_j^H}\mathrm{tr}\left(\widetilde{\boldsymbol{p}}_j\boldsymbol{h}_j^T\boldsymbol{h}_i\widetilde{\boldsymbol{p}}_i^T\right).$$

We note that $e^{\underline{\boldsymbol{A}}(t-s)} = \boldsymbol{Q}e^{\widehat{\boldsymbol{A}}(t-s)}\boldsymbol{Q}^{-1}$ and $E_\zeta^N(\infty) = -\sigma^2\sum_{i=1}^{2(n-1)m}\sum_{j=1}^{2(n-1)m}\frac{\mathrm{tr}(\widetilde{\boldsymbol{p}}_j\boldsymbol{h}_j^T\boldsymbol{h}_i\widetilde{\boldsymbol{p}}_i^T)}{\psi_i+\psi_j^H}$.

Combining the above with the definitions of $\boldsymbol{\xi}(t)$, $\underline{\boldsymbol{\xi}}(t)$, and $\boldsymbol{\zeta}(t)$ enables the evaluation of $\mathbb{E}[\|\boldsymbol{\xi}(t)\|_2^2]$ and $\|\mathbb{E}[\boldsymbol{\xi}(t)]\|_2$, respectively, as

$$\mathbb{E}\left[\|\boldsymbol{\xi}(t)\|_2^2\right] = E_\zeta(t) = E_\zeta^D(t) + E_\zeta^N(t), \tag{17}$$

and

$$\|\mathbb{E}\left[\boldsymbol{\xi}(t)\right]\|_2 = \left\|\mathbb{E}\left[\underline{\boldsymbol{\xi}}(t)\right]\right\|_2 = \|\mathbb{E}\left[\boldsymbol{\zeta}(t)\right]\|_2 = \sqrt{E_\zeta^D(t)}. \tag{18}$$

From the analysis above and Remark A1, it can be shown that $E_\zeta^D(t) \le \lambda_{\max}(\boldsymbol{Q}^H\boldsymbol{Q})e^{2\varphi_{\max}^{\mathrm{re}}t}\|\boldsymbol{Q}^{-1}\boldsymbol{\zeta}(0)\|_2^2$, where $\lambda_{\max}(\cdot)$ denotes the maximum eigenvalue and

$$\varphi_{\max}^{\mathrm{re}} := \max_{1\le i\le (n-1)} \varphi^{\mathrm{re}}(\lambda_i) \tag{19}$$

with $\varphi^{\mathrm{re}}(\lambda)$ defined in (13) such that $\lim_{t\to\infty} E_\zeta^D(t) = 0$, and $E_\zeta^N(t) \le E_\zeta^N(\infty) < \infty$. Hence, $\mathbb{E}[\|\boldsymbol{\xi}(t)\|_2^2] < \infty$, $\|\mathbb{E}[\boldsymbol{\xi}(t)]\|_2 < \infty$, and $\overline{L}_{i,j}(t) < \infty$, such that $C_{\mathrm{ergL}}(\overline{L}_{i,j}(t)) > 0$, and

$$\lim_{t\to\infty}\mathbb{E}\left[\|\boldsymbol{p}_i(t)-\boldsymbol{p}_j(t)\|_2^2\right] \le U_{ij} \tag{20}$$

where

$$U_{ij} = 4E_\zeta^N(\infty) + \|\boldsymbol{\delta}_i - \boldsymbol{\delta}_j\|_2^2. \tag{21}$$

Similarly, it holds that $\mathbb{E}[\|\boldsymbol{v}_i(t)-\boldsymbol{v}_j(t)\|_2^2] \le \overline{L}_{i,j}(t)$, and thus

$$\lim_{t\to\infty}\mathbb{E}\left[\|\boldsymbol{v}_i(t)-\boldsymbol{v}_j(t)\|_2^2\right] \le U_{ij}. \tag{22}$$

Finally, recalling Lemma 3, we can get

$$\lim_{t\to\infty}\mathbb{E}\left[C_{\mathrm{ergL}}\left(\|\boldsymbol{p}_i(t)-\boldsymbol{p}_j(t)\|_2^2\right)\right] \ge C_{\mathrm{ergL}}\left(U_{ij}\right). \tag{23}$$

This completes the proof. ■

Appendix C
Proof of Theorem 3

From the proof of Theorem 2, together with Lemma A1, we get $\overline{L}_{i,j}(t-t_0) - U_{ij} = 4E_\zeta^D(t-t_0) + 4(E_\zeta^N(t-t_0) - E_\zeta^N(\infty)) + 4\|\boldsymbol{\delta}_i - \boldsymbol{\delta}_j\|_2\sqrt{E_\zeta^D(t-t_0)} = O(e^{\varphi_{\max}^{\mathrm{re}}(t-t_0)})$, where $E_\zeta^D(t-t_0) = O(e^{2\varphi_{\max}^{\mathrm{re}}(t-t_0)})$ and $E_\zeta^N(t-t_0) - E_\zeta^N(\infty) = O(e^{\varphi_{\max}^{\mathrm{re}}(t-t_0)})$. Then, applying the standard method of the Taylor series expansion yields

$$C_{\mathrm{ergL}}\left(\overline{L}_{i,j}\left(t-t_0\right)\right) - C_{\mathrm{ergL}}\left(U_{ij}\right) = O\left(e^{\varphi_{\max}^{\mathrm{re}}(t-t_0)}\right). \tag{24}$$

Therefore, we can prove the result. ■

Appendix D
Proof of Remark 2

From the definition of $\boldsymbol{\theta}(t)$ given in (7), we first find that $\boldsymbol{\theta}(t) = (\frac{1}{n}\boldsymbol{1}_n^T\otimes \boldsymbol{I}_{2m})\boldsymbol{x}(t)$. Substituting this into (5) yields $\dot{\boldsymbol{\theta}}(t) = \boldsymbol{A\theta}(t) + (\frac{1}{n}\boldsymbol{1}_n^T\boldsymbol{G}\otimes\boldsymbol{BK})\boldsymbol{w}(t)$; thus, we can get $\boldsymbol{\theta}(t) = e^{\boldsymbol{A}t}\boldsymbol{\theta}(0) + \sigma\int_0^t e^{\boldsymbol{A}(t-s)}(\frac{1}{n}\boldsymbol{1}_n^T\boldsymbol{G}\otimes\boldsymbol{BK})d\mathcal{B}(s)$, where $\boldsymbol{A} := \boldsymbol{\Theta}(0)\boldsymbol{\Phi}(0)\boldsymbol{\Theta}^{-1}(0)$, with $\boldsymbol{\Theta}(0) = [\begin{smallmatrix}1 & 1\\ 0 & -\alpha\end{smallmatrix}]\otimes\boldsymbol{I}_m$, $\boldsymbol{\Phi}(0) = [\begin{smallmatrix}0 & 0\\ 0 & -\alpha\end{smallmatrix}]\otimes\boldsymbol{I}_m$, and $\boldsymbol{\Theta}^{-1}(0) = -\frac{1}{\alpha}[\begin{smallmatrix}-\alpha & -1\\ 0 & 1\end{smallmatrix}]\otimes\boldsymbol{I}_m$.

Since $e^{\boldsymbol{A}t} = \boldsymbol{\Theta}(0)([\begin{smallmatrix}1 & 0\\ 0 & e^{-\alpha t}\end{smallmatrix}]\otimes\boldsymbol{I}_m)\boldsymbol{\Theta}^{-1}(0)$, the metric $\mathbb{E}[\|\boldsymbol{\theta}(t)\|_2^2]$ is easily computed with the help of Lemma A1, by setting $\boldsymbol{H} = \boldsymbol{\Theta}(0)\otimes\boldsymbol{I}_m$ and $\boldsymbol{P} = (\boldsymbol{\Theta}^{-1}(0)\otimes\boldsymbol{I}_m)(\frac{1}{n}\boldsymbol{1}_n^T\boldsymbol{G}\otimes\boldsymbol{BK})$. That is, $\mathbb{E}[\|\boldsymbol{\theta}(t)\|_2^2] = E_\theta^D(t) + E_\theta^N(t)$, where $E_\theta^D(t) = \|\mathbb{E}[\boldsymbol{\theta}(t)]\|_2^2 = \|e^{\boldsymbol{A}t}\boldsymbol{\theta}(0)\|_2^2$ and $E_\theta^N(t) = \sigma^2\mathbb{E}[\|\int_0^t e^{\boldsymbol{A}(t-s)}(\frac{1}{n}\boldsymbol{1}_n^T\boldsymbol{G}\otimes\boldsymbol{BK})d\mathcal{B}(s)\|_2^2]$.

It is obvious that $E_\theta^D(t)$ has a finite upper bound $\|\boldsymbol{\theta}(0)\|_2^2$ such that $E_\theta^D(t) = O(1)$. We can then obtain $E_\theta^N(t) = O(t)$. It therefore suffices to show that the mean square of $\theta(t)$ of the multiagent system goes to infinity due to random errors.

This concludes the proof of Remark 2. ■

References

[1] X. Dong and G. Hu, "Time-varying output formation for linear multiagent systems via dynamic output feedback control," *IEEE Trans. Control Netw. Syst.*, vol. 4, no. 2, pp. 236–245, Jun. 2017.

[2] Z. Li, T. Huang, Y. Tang, and W. Zhang, "Formation control of multiagent systems with communication noise: A convex analysis approach," *IEEE Trans. Cybern.*, to be published, doi: 10.1109/TCYB.2019.2936347.

[3] K. Oh, M. Park, and H. Ahn, "A survey of multi-agent formation control," *Automatica*, vol. 53, pp. 424–440, 2015.

[4] Q. Van Tran *et al.*, "Finite-time bearing-only formation control via distributed global orientation estimation," *IEEE Trans. Control Netw. Syst.*, vol. 6, no. 2, pp. 702–712, Jun. 2019.

[5] S. Zuo, Y. Song, F. L. Lewis, and A. Davoudi, "Time-varying output formation containment of general linear homogeneous and heterogeneous multiagent systems," *IEEE Trans. Control Netw. Syst.*, vol. 6, no. 2, pp. 537–548, Jun. 2019.

[6] Z. Han, L. Wang, Z. Lin, and R. Zheng, "Formation control with size scaling via a complex Laplacian-based approach," *IEEE Trans. Cybern.*, vol. 46, no. 10, pp. 2348–2359, Oct. 2016.

[7] A. Abdessameud and A. Tayebi, "Formation control of VTOL unmanned aerial vehicles with communication delays," *Automatica*, vol. 47, no. 11, pp. 2383–2394, 2011.

[8] M. Huang and J. Manton, "Coordination and consensus of networked agents with noisy measurements: Stochastic algorithms and asymptotic behavior," *SIAM J. Control Optim.*, vol. 48, no. 1, pp. 134–161, 2009.

[9] L. Gupta, R. Jain, and G. Vaszkun, "Survey of important issues in UAV communication networks," *IEEE Commun. Surveys. Tuts.*, vol. 18, no. 2, pp. 1123–1152, Apr.–Jun. 2016.

[10] S. Hayat, E. Yanmaz, and R. Muzaffar, "Survey on unmanned aerial vehicle networks for civil applications: A communications viewpoint," *IEEE Commun. Surveys Tut.*, vol. 18, no. 4, pp. 2624–2661, Oct.–Dec. 2016.

[11] O. Sahingoz, "Networking models in flying ad-hoc networks (FANETs): Concepts and challenges," *J. Intell. Robot. Syst.*, vol. 74, nos. 1/2, pp. 513–527, 2014.

[12] B. Wang and Y. Tian, "Distributed formation control: Asymptotic stabilization results under local noisy information," *IEEE Trans. Cybern.*, to be published, doi: 10.1109/TCYB.2019.2897605.

[13] X. Li and L. Xie, "Dynamic formation control over directed networks using graphical Laplacian approach," *IEEE Trans. Autom. Control*, vol. 63, no. 11, pp. 3761–3774, Nov. 2018.

[14] G. Wen, C. L. P. Chen, and Y.-J. Liu, "Formation control with obstacle avoidance for a class of stochastic multiagent systems," *IEEE Trans. Ind. Electron.*, vol. 65, no. 7, pp. 5847–5855, Jul. 2018.

[15] X. Ge and Q.-L. Han, "Distributed formation control of networked multiagent systems using a dynamic event-triggered communication mechanism," *IEEE Trans. Ind. Electron.*, vol. 64, no. 10, pp. 8118–8127, Oct. 2017.

[16] Z. Lin, L. Wang, Z. Han, and M. Fu, "Distributed formation control of multi-agent systems using complex Laplacian," *IEEE Trans. Autom. Control*, vol. 59, no. 7, pp. 1765–1777, Jul. 2014.
[17] S. Chandrasekharan *et al.*, "Designing and implementing future aerial communication networks," *IEEE Commun. Mag.*, vol. 54, no. 5, pp. 26–34, May 2016.
[18] Y. Zeng, R. Zhang, and T. J. Lim, "Wireless communications with unmanned aerial vehicles: Opportunities and challenges," *IEEE Commun. Mag.*, vol. 54, no. 5, pp. 36–42, May 2016.
[19] Z. Yuan *et al.*, "Ultra-reliable IoT communications with UAVs: A swarm use case," *IEEE Commun. Mag.*, vol. 56, no. 12, pp. 90–96, Dec. 2018.
[20] M. Mozaffari, W. Saad, M. Bennis, and M. Debbah, "Efficient deployment of multiple unmanned aerial vehicles for optimal wireless coverage," *IEEE Commun. Lett.*, vol. 20, no. 8, pp. 1647–1650, Aug. 2016.
[21] X. Yuan *et al.*, "Capacity analysis of UAV communications: Cases of random trajectories," *IEEE Trans. Veh. Technol.*, vol. 67, no. 8, pp. 7564–7576, Aug. 2018.
[22] T. Ernest, A. Madhukumar, R. Sirigina, and A. Krishna, "Outage analysis and finite SNR diversity-multiplexing tradeoff of hybrid-duplex systems for aeronautical communications," *IEEE Trans. Wireless Commun.*, vol. 18, no. 4, pp. 2299–2313, Apr. 2019.
[23] T. Li and J. Zhang, "Mean square average consensus under measurement noises and fixed topologies: Necessary and sufficient conditions," *Automatica*, vol. 45, no. 8, pp. 1929–1936, 2009.
[24] T. Li and J. Zhang, "Consensus conditions of multi-agent systems with time-varying topologies and stochastic communication noises," *IEEE Trans. Autom. Control*, vol. 55, no. 9, pp. 2043–2057, Sep. 2010.
[25] Z. Li and J. Chen, "Robust consensus of multi-agent systems with stochastic uncertain channels," in *Proc. Amer. Control Conf.*, 2016, pp. 3722–3727.
[26] X. Ma and N. Elia, "Mean square performance and robust yet fragile nature of torus networked average consensus," *IEEE Trans. Control Netw. Syst.*, vol. 2, no. 3, pp. 216–225, Sep. 2015.
[27] K. You and L. Xie, "Network topology and communication data rate for consensusability of discrete-time multi-agent systems," *IEEE Trans. Autom. Control*, vol. 56, no. 10, pp. 2262–2275, Oct. 2011.
[28] N. Goddemeier, K. Daniel, and C. Wietfeld, "Role-based connectivity management with realistic air-to-ground channels for cooperative UAVs," *IEEE J. Sel. Areas Commun.*, vol. 30, no. 5, pp. 951–963, Jun. 2012.
[29] J. Baillieul and P. Antsaklis, "Control and communication challenges in networked real-time systems," *Proc. IEEE*, vol. 95, no. 1, pp. 9–28, Jan. 2007.
[30] I. Lestas, "Power control in wireless networks: stability and delay independence for a general class of distributed algorithms," *IEEE Trans. Autom. Control*, vol. 57, no. 5, pp. 1253–1258, May 2012.
[31] N. Elia, "When Bode meets Shannon: Control-oriented feedback communication schemes," *IEEE Trans. Autom. Control*, vol. 49, no. 9, pp. 1477–1488, Sep. 2004.
[32] N. Martins and M. Dahleh, "Feedback control in the presence of noisy channels: "Bode-like fundamental" limitations of performance," *IEEE Trans. Autom. Control*, vol. 53, no. 7, pp. 1604–1615, Aug. 2008.
[33] S. Tatikonda and S. Mitter, "Control under communication constraints," *IEEE Trans. Autom. Control*, vol. 49, no. 7, pp. 1056–1068, Jul. 2004.
[34] G. Nair and R. Evans, "Stabilizability of stochastic linear systems with finite feedback data rates," *SIAM J. Control Optim.*, vol. 43, no. 2, pp. 413–436, 2004.
[35] P. Minero, M. Franceschetti, S. Dey, and G. Nair, "Data rate theorem for stabilization over time-varying feedback channels," *IEEE Trans. Autom. Control*, vol. 54, no. 2, pp. 243–255, Feb. 2009.
[36] T. Tanaka, P. Esfahani, and S. Mitter, "LQG control with minimum directed information: Semidefinite programming approach," *IEEE Trans. Autom. Control*, vol. 63, no. 1, pp. 37–52, Jan. 2018.
[37] W. Wong and R. Brockett, "Systems with finite communication bandwidth constraints—II: Stabilization with limited information feedback," *IEEE Trans. Autom. Control*, vol. 44, no. 5, pp. 1049–1053, May 1999.
[38] J. Braslavsky, R. Middleton, and J. Freudenberg, "Feedback stabilisation over signal-to-noise ratio constrained channels," *IEEE Trans. Autom. Control*, vol. 52, no. 8, pp. 1391–1403, Aug. 2007.
[39] N. Martins, M. Dahleh, and N. Elia, "Feedback stabilization of uncertain systems in the presence of a direct link," *IEEE Trans. Autom. Control*, vol. 51, no. 3, pp. 438–447, Mar. 2006.
[40] A. Sahai and S. Mitter, "The necessity and sufficiency of anytime capacity for stabilization of a linear system over a noisy communication link—Part I: Scalar systems," *IEEE Trans. Inf. Theory*, vol. 52, no. 8, pp. 3369–3395, Aug. 2006.
[41] G. Ranade and A. Sahai, "Control capacity," *IEEE Trans. Inf. Theory*, vol. 65, no. 1, pp. 235–254, Jan. 2019.
[42] V. Kostina and B. Hassibi, "Rate-cost tradeoffs in control," *IEEE Trans. Autom. Control*, vol. 64, no. 11, pp. 4525–4540, Nov. 2019.
[43] E. Haas, "Aeronautical channel modeling," *IEEE Trans. Veh. Technol.*, vol. 51, no. 2, pp. 254–264, Mar. 2002.
[44] W. Ren, "Consensus strategies for cooperative control of vehicle formations," *IET Control Theory Appl.*, vol. 1, no. 2, pp. 505–512, Mar. 2007.
[45] X. Ai, S. Song, and K. You, "Second-order consensus of multi-agent systems under limited interaction ranges," *Automatica*, vol. 68, pp. 329–333, 2016.
[46] L. Cheng, Z. Hou, M. Tan, and X. Wang, "Necessary and sufficient conditions for consensus of double-integrator multi-agent systems with measurement noises," *IEEE Trans. Autom. Control*, vol. 56, no. 8, pp. 1958–1963, Aug. 2011.
[47] S. P. Nandanoori, A. Diwadkar, and U. Vaidya, "Mean square stability analysis of stochastic continuous-time linear networked systems," *IEEE Trans. Autom. Control*, vol. 63, no. 12, pp. 4323–4330, Dec. 2018.
[48] G. Chen, "Small noise may diversify collective motion in Vicsek model," *IEEE Trans. Autom. Control*, vol. 62, no. 2, pp. 636–651, Feb. 2017.
[49] T. Vicsek and A. Zafeiri, "Collective Motion," *Phys. Rep.*, vol. 517, no. 3, pp. 71–140, 2012.
[50] R. Merris, "Laplacian matrices of graphs: A survey," *Linear Algebra Appl.*, vol. 197, no. 1, pp. 143–176, 1994.
[51] M. Conti and S. Giordano, "Mobile ad-hoc networking: Milestones, challenges, and new research directions," *IEEE Commun. Mag.*, vol. 52, no. 1, pp. 85–96, Jan. 2014.
[52] I. Bekmezci, O. Sahingoz, and S. Temel, "Flying ad-hoc networks (FANETs): A survey," *Ad Hoc Netw.*, vol. 11, no. 3, pp. 1254–1270, May 2013.
[53] C. Marco, "Multihop ad-hoc networking: The theory," *IEEE Commun. Mag.*, vol. 45, no. 4, pp. 78–86, Apr. 2007.
[54] S. Rosati *et al.*, "Dynamic routing for flying ad-hoc networks," *IEEE Trans. Veh. Technol.*, vol. 65, no. 3, pp. 1690–1700, Mar. 2016.
[55] S. Fang, J. Chen, and H. Ishii, *Towards Integrating Control and Information Theories: From Information-Theoretic Measures to Control Performance Limitations* (Lecture Notes in Control and Information Sciences). Cham, Switzerland: Springer, 2017.
[56] Z. Li and Z. Duan, *Cooperative Control of Multi-Agent Systems: A Consensus Region Approach*. New York, NY, USA: Taylor & Francis/CRC Press, 2014.
[57] A. Goldsmith, *Wireless Communications*. Cambridge, U.K.: Cambridge Univ. Press, 2005.
[58] B. Oksendal, *Stochastic Differential Equations—An Introduction with Applications*. Berlin, Germany: Springer, 1998.
[59] J. Proakis and M. Saleh, *Digital Communications*, 5th ed. New York, NY, USA: McGraw-Hill, 2008.
[60] C. Chen, *Linear System Theory and Design*, 3rd ed. New York, NY, USA: Oxford Univ. Press, 1999.

Rongrong Qian (Member, IEEE) received the B.S. degree in communication engineering and the Ph.D. degree in signal and information processing from the Beijing University of Posts and Telecommunication (BUPT), Beijing, China, in 2004 and 2010, respectively.

From 2010 to 2020, he was a Lecturer and Associate Professor with the Automation School, BUPT. He is currently an Associate Professor with the School of Artificial Intelligence, BUPT. From 2015 to 2016, he was a Visiting Scholar with the College of Engineering, Peking University, Beijing, China. His research interests include control-communication integrated theory and techniques with applications to multi-UAV systems and signal processing in wireless communications.

Zhisheng Duan (Senior Member, IEEE) received the M.S. degree in mathematics from Inner Mongolia University, Hohhot, China, and the Ph.D. degree in control theory from Peking University, Beijing, China, in 1997 and 2000, respectively.

From 2000 to 2002, he was a Postdoctor with Peking University. Since 2008, he has been a Professor with the Department of Mechanics and Aerospace Engineering, College of Engineering, Peking University. He obtained the Outstanding Youth Fund of National Natural Science, in 2012. He is currently a Changjiang Scholar with Peking University. His research interests include robust control, stability of interconnected systems, and analysis and control of complex dynamical networks.

Dr. Duan was the recipient of the 2001 Chinese Control Conference Guan-Zhaozhi Award, the 2011 First Class Award in Natural Science from the Chinese Ministry of Education, and the 2015 Second Class Award of National Natural Science.

Yuan Qi (Member, IEEE) received the B.S. degree in communication engineering and the Ph.D. degree in signal and information processing from the Beijing University of Posts and Telecommunication (BUPT), Beijing, China, in 2004 and 2009, respectively.

Since 2009, she has been a Lecturer with the School of Electronic Engineering, BUPT. Her research interests include millimeter-wave communications, multi-input–multi-output (MIMO) systems, and signal processing in wireless communications.

Tao Peng (Member, IEEE) received the B.S. degree in communication engineering and the M.S. and Ph.D. degrees in signal and information processing from the Beijing University of Posts and Telecommunication (BUPT), Beijing, China, in 1999, 2002, and 2010, respectively.

He is currently an Associate Professor with BUPT, where he has been the Chair of Device-to-Device (D2D) Technical Discussion Group of IMT-A/IMT-2020 Propulsion Group in CCSA. He has authored more than 70 academic papers with 16 SCI indexed, and is the inventor of 25 international and domestic patents. His research interests include cognitive radio and software defined radio, D2D communication, CRAN and ultradense networks, and mobile ad-hoc networks.

Wenbo Wang (Senior Member, IEEE) received the B.S. degree in communication engineering and the M.S. and Ph.D. degrees in signal and information processing from the Beijing University of Posts and Telecommunications (BUPT), Beijing, China, in 1986, 1989, and 1992, respectively.

From 1992 to 1993, he was a Researcher with ICON Communication Inc., Dallas, TX, USA. He has been a Chair Professor with the School of Information and Communications Engineering, BUPT, where he is currently the Vice-President of BUPT. He is also the Assistant Director of the Universal Wireless Communication Laboratory. He has also been the Director of the Beijing Institute of Communication, since 2002, and an Assistant Director of the National Defense Communication Committee, China Institute of Communication. He has authored or coauthored more than 200 articles, six books and holds 12 patents. His research interests include transmission technology, broadband wireless access, wireless network theory, digital signal processing, mutiple-input–multiple output (MIMO), cooperative and cognitive communications, and software radio technology.